1.0

1.1

1.25

2.8

3.2

3.6

1.4

2.5

2.2

2.0

1.8

1.6

MICROCOPY RESOLUTION TEST CHART

AD-E200 467

②**LEVEL** Ⅲ

DIELECTRIC GUIDE CONTROLLED COLLECTIVE ION ACCELERATION

Spire Corporation
Patriots Park
Bedford, MA 01730

February 1980

Final Report

Approved for public release; distribution unlimited.

DTIC
ELECTE
JUN 3 1980
S   D
B

AIR FORCE WEAPONS LABORATORY
Air Force Systems Command
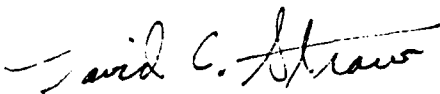Kirtland Air Force Base, NM 87117

80 3 17 071

This final report was prepared by the Spire Corporation, Bedford, Massachusetts, under Contract F29601-77-C-0081, Job Order 2301Y102 with the Air Force Weapons Laboratory, Kirtland Air Force Base, New Mexico. Dr. David C. Straw (NTYP) was the Laboratory Project Officer-in-Charge.

When US Government drawings, specifications, or other data are used for any purpose other than a definitely related Government procurement operation, the Government thereby incurs no responsibility nor any obligation whatsoever, and the fact that the Government may have formulated, furnished, or in any way supplied the said drawings, specifications, or other data, is not to be regarded by implication or otherwise, as in any manner licensing the holder or any other person or corporation, or conveying any rights or permission to manufacture, use, or sell any patented invention that may in any way be related thereto.

This report has been authored by a contractor of the United States Government. The United States Government retains a nonexclusive, royalty-free license to publish or reproduce the material contained herein, or allow others to do so, for the United States Government purposes.

This report has been reviewed by the Public Affairs Office and is releasable to the National Technical Information Service (NTIS). At NTIS, it will be available to the general public, including foreign nations.

This technical report has been reviewed and is approved for publication.
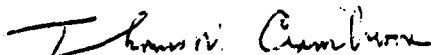
DAVID C. STRAW, PhD
Project Officer

FOR THE DIRECTOR

NORMAN F. RODERICK
Lt Colonel, USAF
Chief, Advanced Concepts Branch

THOMAS W. CIAMBRONE
Colonel, USAF
Chief, Applied Physics Division

REPORT DOCUMENTATION PAGE	READ INSTRUCTIONS BEFORE COMPLETING FORM

1. REPORT NUMBER AFWL-TR-77-248	2. GOVT ACCESSION NO. AD-A084994	3. RECIPIENT'S CATALOG NUMBER

4. TITLE (and Subtitle) DIELECTRIC GUIDE CONTROLLED COLLECTIVE ION ACCELERATION.	5. TYPE OF REPORT & PERIOD COVERED Final Report
	6. PERFORMING ORG. REPORT NUMBER FR-60015

7. AUTHOR(s)	8. CONTRACT OR GRANT NUMBER(s) F29601-77-C-0081

9. PERFORMING ORGANIZATION NAME AND ADDRESS Spire Corporation Patriots Park Bedford, MA 01730	10. PROGRAM ELEMENT. PROJECT, TASK AREA & WORK UNIT NUMBERS 61601F/2301Y102

11. CONTROLLING OFFICE NAME AND ADDRESS Air Force Weapons Laboratory (NTYP) Kirtland Air Force Base, NM 87117	12. REPORT DATE February 1980
	13. NUMBER OF PAGES 48

14. MONITORING AGENCY NAME & ADDRESS(if different from Controlling Office)	15. SECURITY CLASS. (of this report) Unclassified
	15a. DECLASSIFICATION. DOWNGRADING SCHEDULE

16. DISTRIBUTION STATEMENT (of this Report)

Approved for public release; distribution unlimited.

17. DISTRIBUTION STATEMENT (of the abstract entered in Block 20, if different from Report)

18. SUPPLEMENTARY NOTES

19. KEY WORDS (Continue on reverse side if necessary and identify by block number)

Unconventional Accelerators
Collective Effect Acceleration
Dielectric Guide Control

20. ABSTRACT (Continue on reverse side if necessary and identify by block number)

Experiments performed at Spire and at NRL have demonstrated dielectric guide controlled collective ion acceleration. Control of the phenomenon has been established by varying the electron beam parameters or guide geometry. Specifically, it has been shown that: Total electron current must exceed the space charge limit; increasing electron current density increases the ion energy; a minimum electron current density is required; increasing guide length (assuming the electron beam can propagate to the end) increases ion energy; increasing guide radius at constant electron current decreases ion energy; and, the energy

DD FORM 1473
1 JAN 73

or charge deposited per unit area of wall controls the velocity of propagation of the electron beam front and therefore the energy of the ions. NRL VEBA results showed that: Dielectric guide controlled collective ion acceleration is effective at higher electron beam energies; an electron beam with current pinched on axis is more efficient for ion acceleration; and molding the surface of the guide can control the beam front velocity.

TABLE OF CONTENTS

ACCESSION for

NTIS   White Section ☑
DDC   Buff Section ☐
UNANNOUNCED   ☐
JUSTIFICATION ....

BY
DISTRIBUTION/AVAILABILITY CODES

Dist.	AVAIL. and/or SPECIAL
A	

LIST OF ILLUSTRATIONS

SECTION I

INTRODUCTION

Conventional ion accelerators are physically limited to accelerating fields on the order of 10^4 volts/cm. Experiments[1] with collective ion acceleration using the space charge wells of IREB (intense relativistic electron beams) have demonstrated accelerating fields exceeding 10^6 V/cm. New applications are possible with the development of compact, lightweight, low cost collective effect ion accelerators.

Problems in controlling collective ion acceleration mechanisms [2] have limited the effective length over which the ions gain energy. Programs[3] in this field have sought to demonstrate the required control. This project has shown that control of the potential well velocity of an IREB can be achieved by placing a dielectric liner in the evacuated accelerating cavity. Experiments were performed with peak electron energies ≈ 100 keV. Scaling laws were developed to show how the phenomenon scales to energy ranges of interest. An independent experiment[4] has verified these scaling laws at electron energies of 1.5 to 2.0 MeV and demonstrated collective ion acceleration to 15 MeV in 15 cm.

This report summarizes the experiments performed at Spire Corporation facilities and presents an analytical model of the phenomenon. Scaling laws derived from this model are then shown to apply to experiments at more than one order of magnitude increase in energy. Diagnostics to determine ion energy, developed under this program, are also discussed.

3

SECTION II
EXPERIMENTS AT SPIRE FACILITIES

2.1 DESCRIPTION

A schematic of the experimental apparatus is shown in Figure 1. A pulsed power source (charged transmission line) is connected to a field emission diode consisting of a planar cathode and transparent mesh anode. The electron beam emitted from the diode is injected into a plastic cylinder, which is referred to as a dielectric guide. The guide is inside a vacuum tank which has conducting walls. Diagnostics to measure the electron or ion beam characteristics are placed at the end of the guide.

The current in the electron beam exceeds the space charge limiting value and the beam does not propagate axially. It blows up radially and impinges upon the walls of the vacuum chamber (Figure 2a). Bombardment by intense radiation causes the release of ions from the plastic material (Figure 2b). Positive ions are drawn into the drift chamber by the space charge fields of the IREB. The strong electric fields are partially neutralized by the positive charge, and the beam propagates axially to an ion-poor region (Figure 2c) where the process is repeated. Ions emitted near the beginning of the guide can be accelerated axially at the beam front to high energies.

To model this phenomenon, electron beam propagation and ion acceleration were studied as functions of:

> Electron beam parameters
> - Particle energy
> - Current density
> - Pulse Width
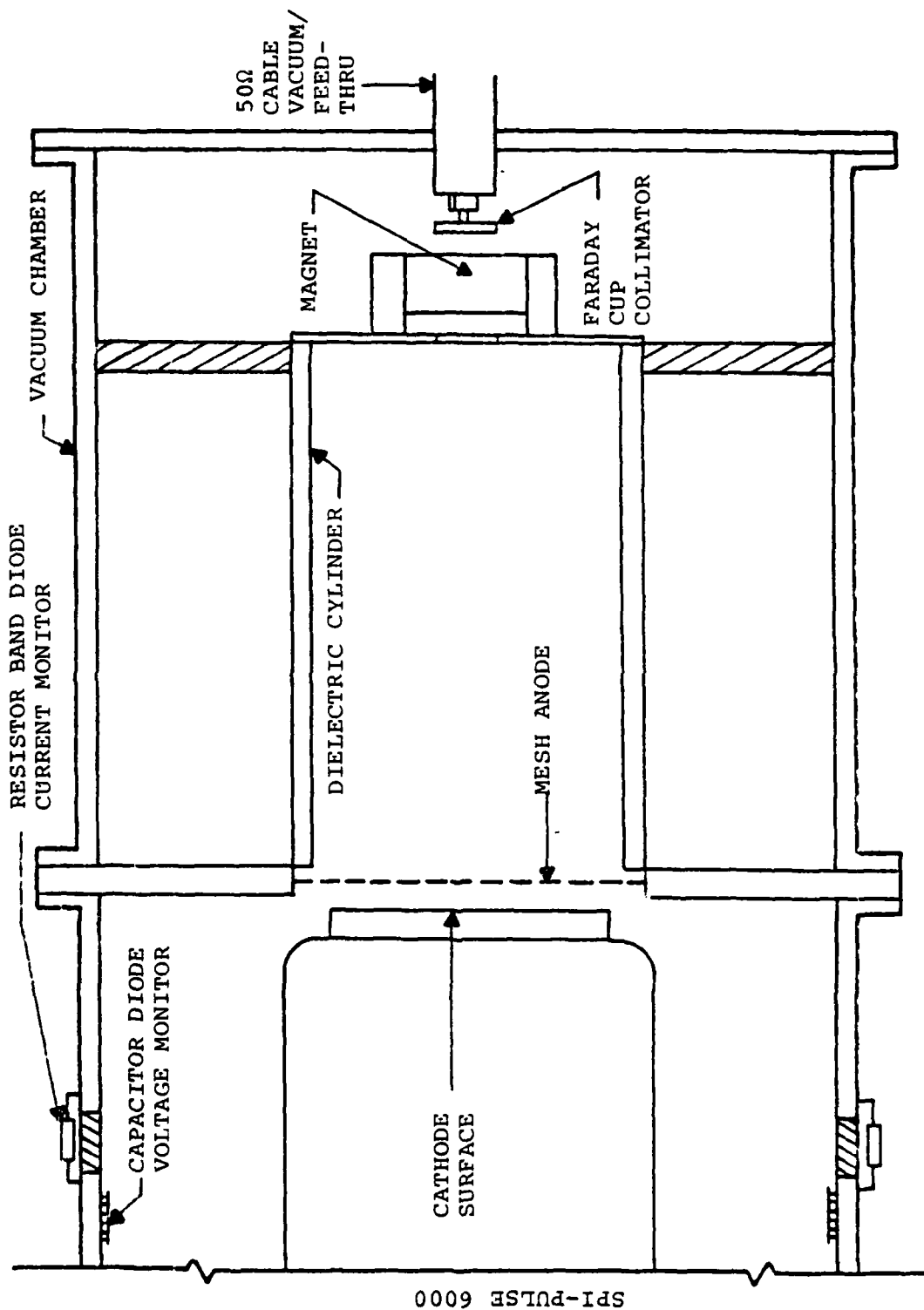
4
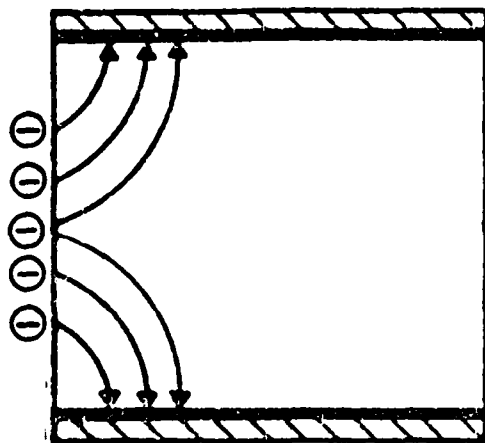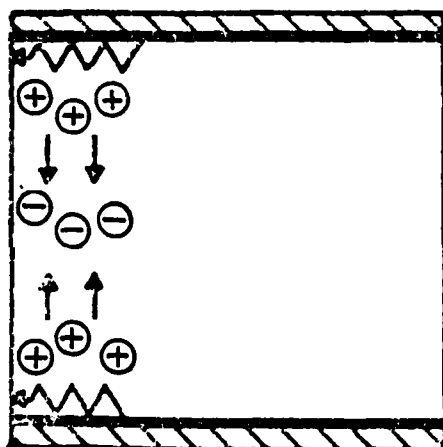
Figure 1. Apparatus for Ion Acceleration Experiment with
Dielectric Cylinder Beam Guide.

5

a

- $\sim \frac{2}{3}$ $Q_{INJ.}$ HITS THE WALL EARLY

- VOLTAGE BUILDS UP

b

- FLASHOVER OCCURS
    — IONS RELEASED

- IONS ACCELERATED INTO CAVITY — SPACE-CHARGE NEUTRALIZE
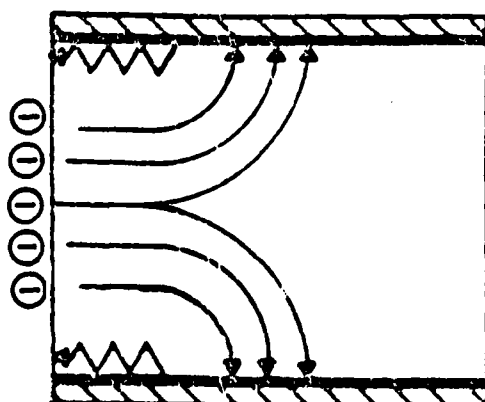
c

- PROCESS REPEATS FURTHER DOWN THE CAVITY UNTIL

    — REACHES END
    — OR NO MORE ELECTRONS

Figure 2. Model.

6

Dielectric guide geometry

- Diameter of cylindrical guide
- Length of cylindrical guide
- Ratio of guide radius to wall radius

The results showed that the ion velocity increased with guide length. The velocity also scaled with injected current density, which could be varied by changing the transmission of the anode or the diameter of the cathode and guide. There were no accelerated ions when the electron beam did not propagate; but the electron beam could propagate without accelerating ions. The effect was linked to the potential well depth.

2.2   DIAGNOSTICS

Two sets of diagnostics were used for these experiments. One set measured electron beam parameters. Another set measured the ion beam parameters.

The electron beam diagnostics were:

- Diode voltage monitor.
- Diode current monitor.
- Axial mounted Faraday cup.
- Return current shunt in outer conducting wall.
- B loops near outer conducting wall.

Of these diagnostics the first three were used most often. The last two diagnostics were mounted in a large radius chamber and were less useful due to restrictions on guide length ($L \approx 2R_{wall}$).

The ion beam diagnostics were:

- Axially mounted Faraday cup

- Screen detector (used with above for
  time-of-flight [TOF] velocity
  measurements.)
- Thin foils for range analysis.
- Nuclear activation analysis.

All diagnostics, except the last, were mounted behind an 800 gauss magnet with 1/4 inch to 1/2 inch diameter apertures on both sides. This magnet separated the ion-electron beams.

Nuclear activation of carbon foils did not require the magnet. The reaction $^{12}C(p,\gamma)^{13}N(\beta^+)^{13}C$ was used. The analysis was unsuccessful because the ion yield above the 457 keV threshold was insufficient ($<10^{11}$ ions) to give a statistically significant count above background. This was a limitation of the low electron energy available at Spire facilities.

The ion current detectors, both a flat plate (Faraday cup) and screen, were isolated from ground and connected to the AC input of an oscilloscope using 50 ohm coax cable. The minimum current which could be detected was 1 mA and was limited by noise. Actual signal strength from a collimated beam was 100 mA on good shots.

One factor contributing to noise was secondary electron emission from the ion collecting plate. To measure this a grounded screen was placed in front of the detector. The collecting plate was biased to ± 90V relative to the screen. The resulting signals are shown in Figure 3. Negative bias forced low energy electrons away from the collector and enhanced the positive signal. Positive bias forced secondary electrons to remain in the collector and did not enhance the

8

Bias
Voltage

−45 V

0

+45 V

+90 V
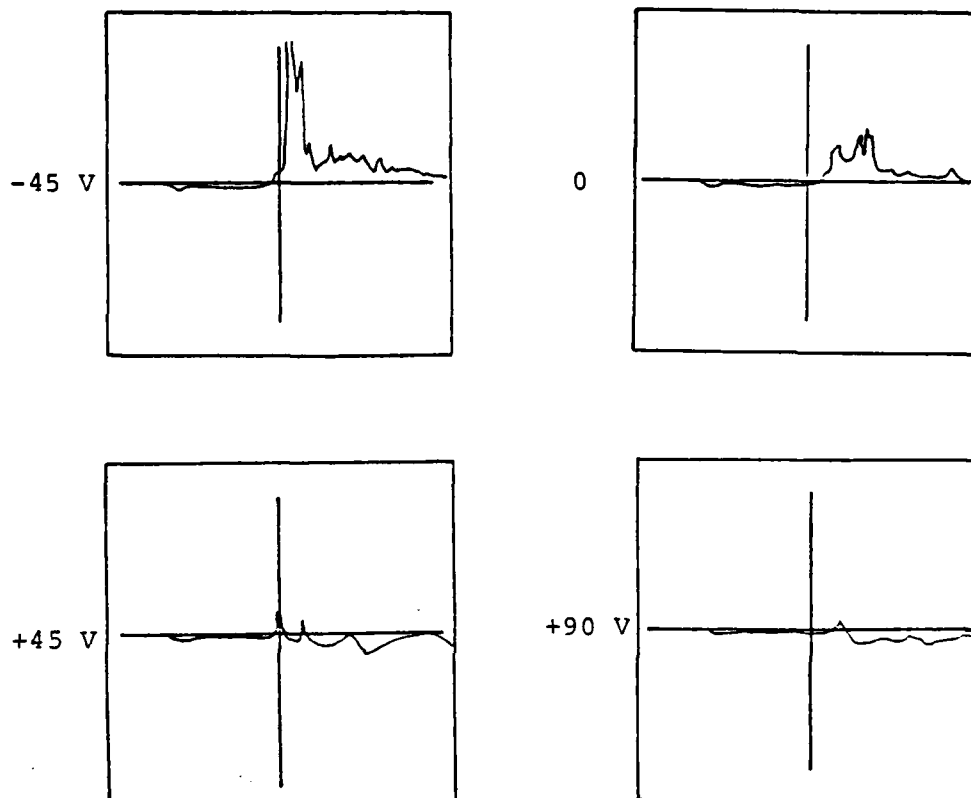
Figure 3.   Effect of Bias Voltage on
             Faraday Cup Ion Signal.

Scales for all traces are 20mV/cm (vertical) and
20ns/cm (horizontal). The collector was behind
a 0.25 inch aperture with a 50 ohm impedence. The
signal increase is due to removal of secondary
electrons from collector plate.

positive signal. Thus, the first positive pulse from an un-
biased ion current collector should represent only positive
ions.

Confirmation that the first positive pulse represented
accelerated ions is shown in Figure 4. The particle beam that
emerged from the (0.5 inch) apertures and magnet at the end of
the dielectric guide (Figure 1) was passed through the screen
detector, 0.1 mil mylar film, and into the solid flat plate
collector. Only the first pulse in the top trace is seen in
the bottom trace with a time delay appropriate for the spacing
between detectors. The pulse width has been increased by scat-
tering, but the range through thin foils corresponds to protons
with an energy consistent with the measured ion velocity
(Figure 5).

2.3   TESTS OF ELECTRON BEAM PARAMETER VARIATION

The following experimental parameters were varied:

- Transmission line length (pulse generator)
- Charging voltage on energy storage
  capacitor
- Cathode radius
- Anode-cathode (A-K) gap
- Anode transparency

Changing these parameters altered the following electron beam
parameters; but not independently.

- Electron energy spectrum
- Total current injected into the
  dielectric guide
- Current density
- Pulse width

10

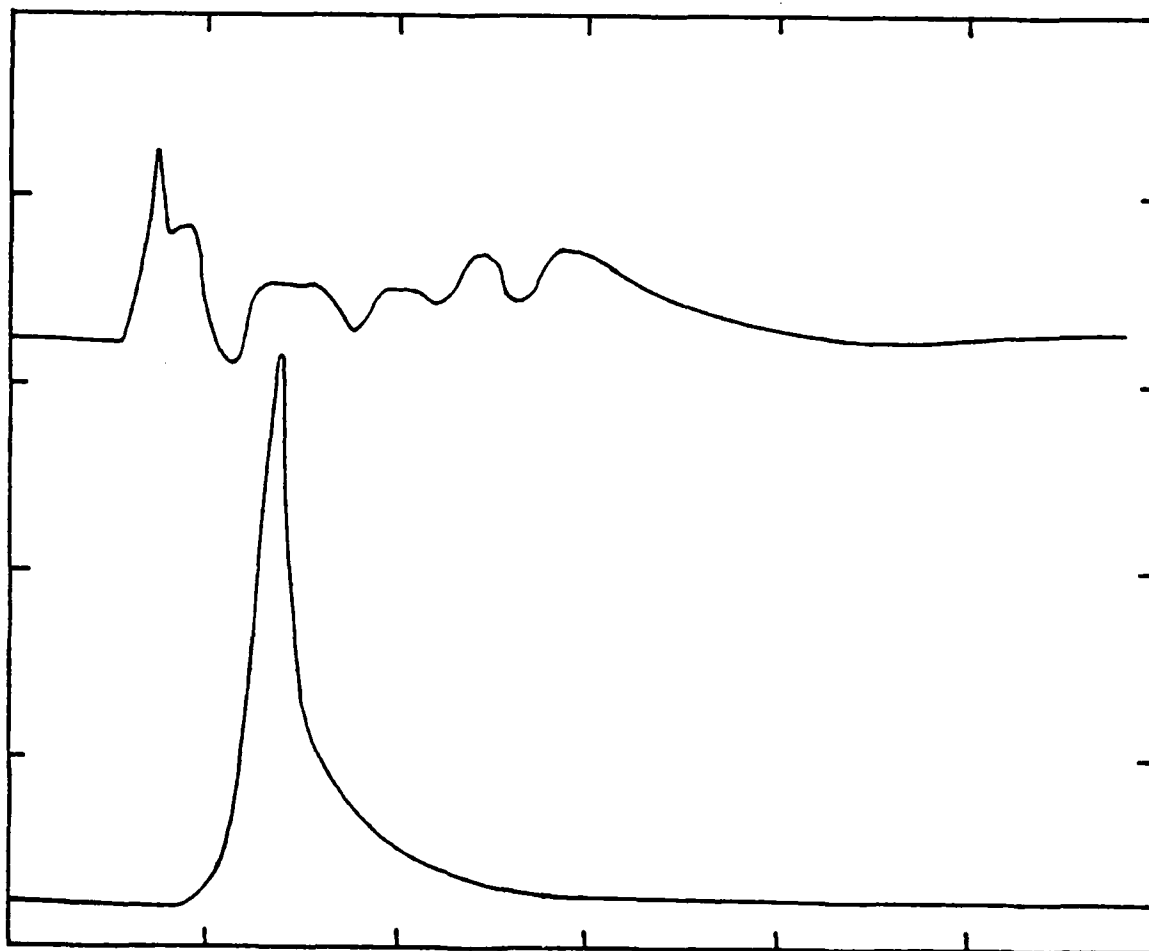Figure 4.   Ion Pulse through 0.1 mil Mylar. Top Trace:
             Initial Pulse, 50ns/division, 100mA/division
             Bottom Trace: After Mylar, 50ns/ division,
             4mA/division. The timing of the traces is
             correlated. Normal delay without mylar would
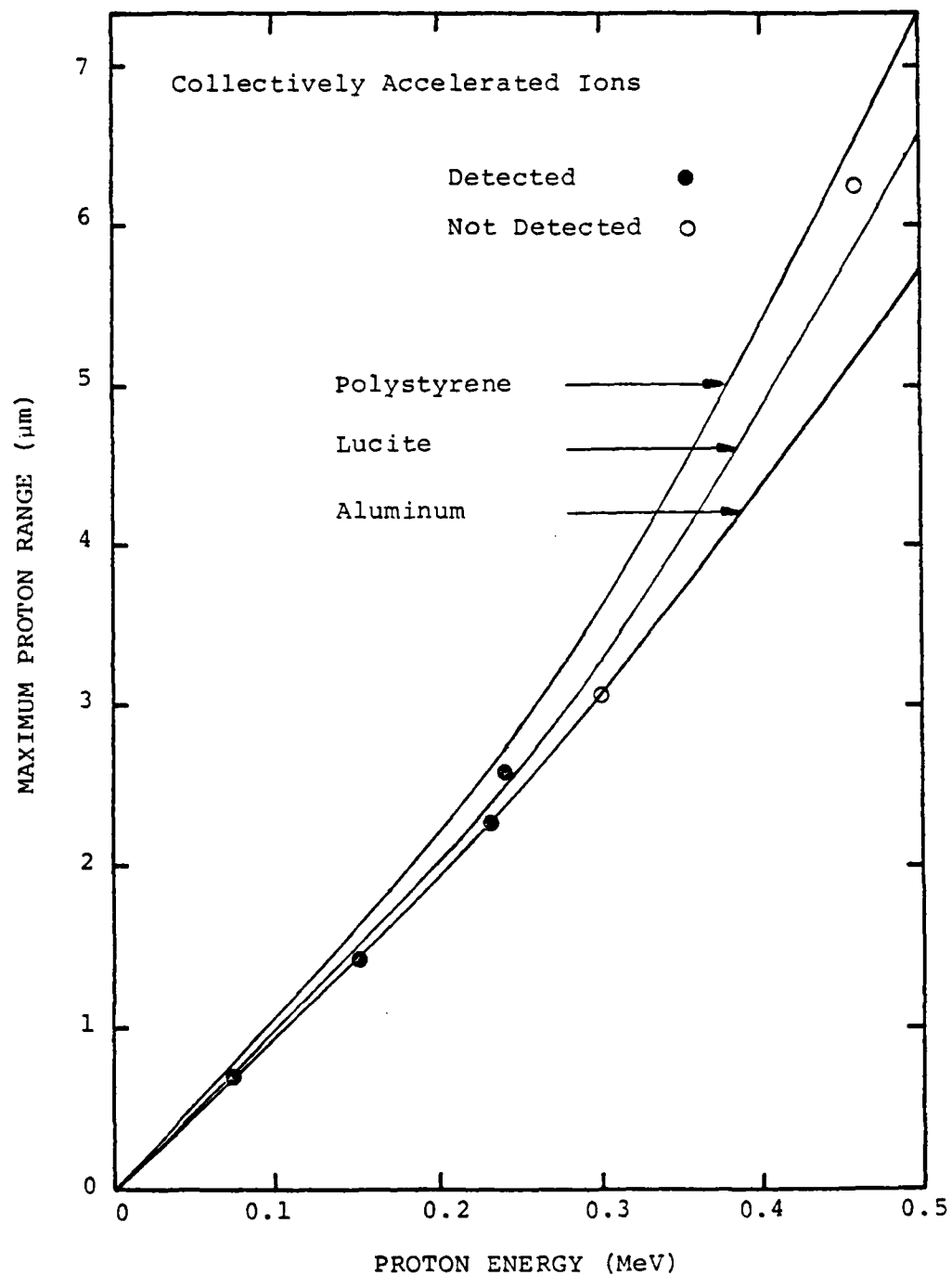   be 10ns from 10cm difference between detectors.

Figure 5.   Maximum Proton Range in Foils.

This study showed that high current density, high impedence electron beams were optimal for ion acceleration.

Early experiments [5] used an REB with a pulse width of approximately 100 ns (Figure 6). As higher energy ions were observed using higher impedence diodes [6] with long pulse widths, the transmission line of the pulse generator was modified to produce an electron beam with a 500 ns pulse width (Figure 7). The electron beams from these two configurations are compared in Table 1. The dielectric guide and cathode radius were reduced with the longer pulse to maintain a high current density and to improve reproducibility.

No accelerated ions were observed with this long pulse. The transmission of the electron beam was reduced in this geometry. The guide (Figure 1) was 1.9 cm I.D. and 2.5 cm O.D. and 10 to 15 cm long. It was placed in a 40 cm I.D. evacuated chamber with conducting walls. The space charge limiting current (for 83 keV electrons) is only $\approx$100 amperes (from equation 1 in section IV of this report) and this value is exceeded by the REB in less than 20 ns. Assuming that all of the current not transmitted to the end of the guide was lost to the walls of the guide, the charge and energy per unit area of dielectric guide wall required to create a sufficient number of positive ions to initiate transport was approximately 1.6 coul/cm^2 and 0.01 cal/cm^2 respectively. For shorter pulse widths these figures are 0.5 coul/cm^2 and 0.01 cal/cm^2.

The conclusion from this experiment was that the removal of positive ions from an acrylic surface by electron bombardment appeared to be *energy dependent at low dose rates.* This implied a thermal mechanism. However, at high energies (Section 4.6) the charge per unit area dominated the mechanism.

13
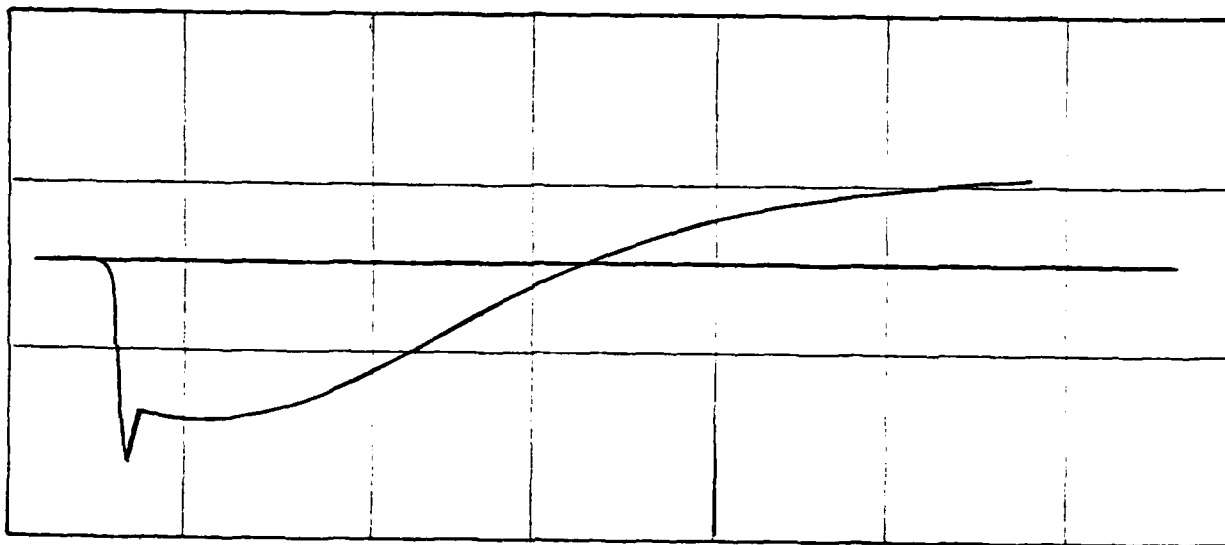
Diode 89.7 kV / division
Voltage 50 ns / division

Figure 6.   Standard Pulse.
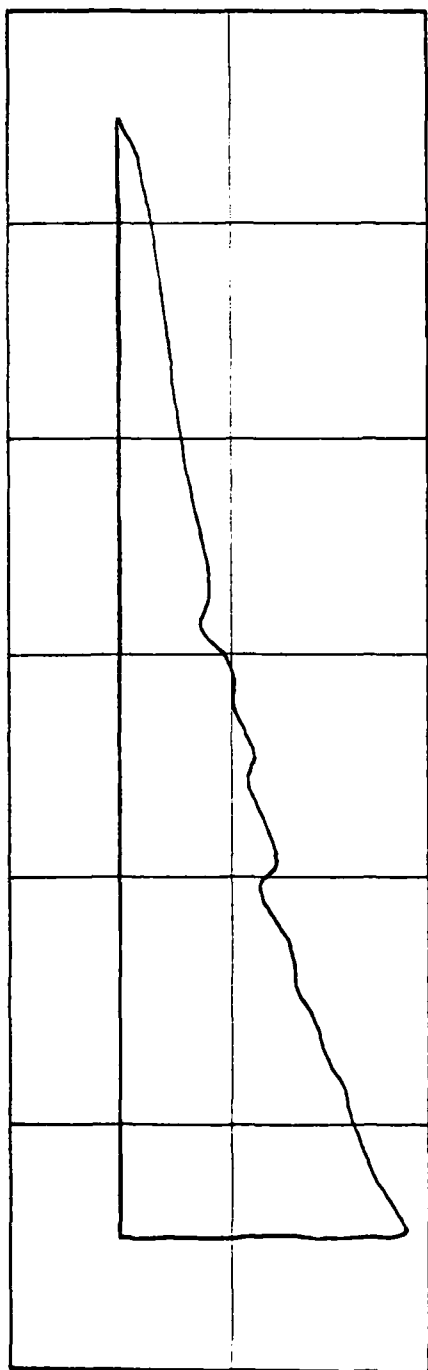
Diode Voltage 62.5 kV, 100 ns per division
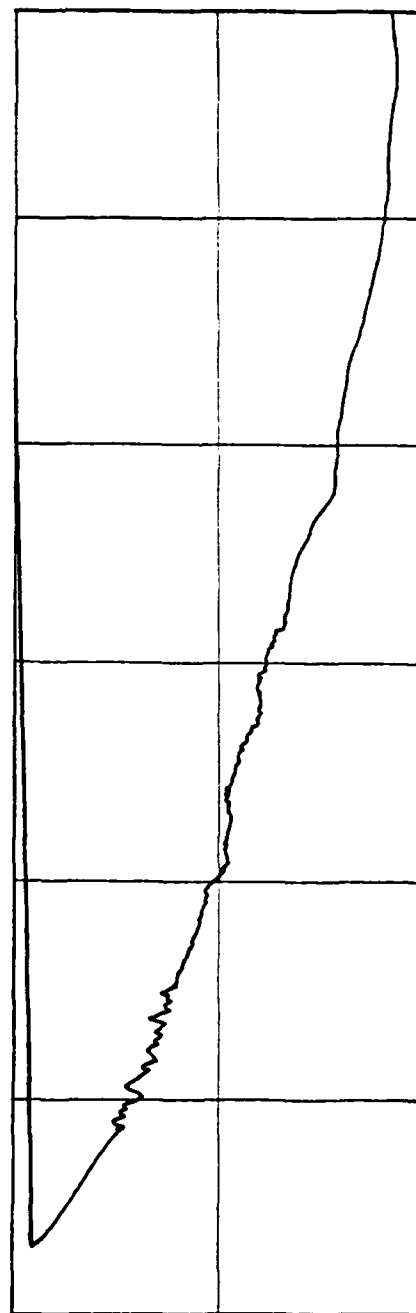
Diode Current 1.2 kA, 100 ns per division

Figure 7.   Long Pulse Diode Characteristics.

15

Table 1

DIODE PARAMETERS USED FOR ION ACCELERATION

Pulse Gener-ator	Charge Voltage kV	Cath. Radius cm	A-K gap cm	Diode Voltage kV †	Diode Current kA †	ν/γ	Total Energy joules	Total Charge mCoul	Pulse Width ns
2500	100	2.5	1.0	83	2.3	0.1	25	1.0	500
5000	150	5.1	0.5	74	12	2.0	75	1.5	130
6000	200	7.6	0.8	130	11	1.2	129	1.5	180

Maximum Values Not Occurring at the Same Time.

†All measurements of voltage and current in the diode are accurate to $\pm$ 5%, see reference 18 for calibration proceedure.

16

Increasing the charging voltage on the energy storage capacitor increased both the average and peak electron energy and the total current. For a constant beam diameter (5.1 cm with a fast pulse) the increased energy density at the anode caused rapid failure of the mesh and increased noise at the ion detector. Lack of reproducibility limited further experiments to larger diameter cathodes. The diameter was changed from 5.1 cm to 7.6 cm and the guide diameter was also increased from 5.7 cm to 7.9 cm. For the parameters in Table 1 the space charge limited current was increased to approximately 400 A, which is still much smaller than the current injected into the guide. The current propagated through 50 cm was 1.5 kA but no accelerated ions were detected. This was believed to be the result of low current density. In Figure 8 this experiment produced the zero point.

Increasing the A-K gap increased the accelerated ion energy [6] for two reasons. At low values of ν/γ the electron beam transport efficiency increased, thus accelerating the ions over a greater length. Also, the electron energy increased (and total beam energy) at large A-K gaps. As long as the beam current exceeded the space charge limiting value, the potential well depth increased with electron energy so the ion energy also increased. All experiments in this study used the largest A-K gap consistent with reproducible beams.

The current injected into the dielectric guide was varied by changing the relative transparency of the mesh anode. Two types of mesh were used: tungsten wire 4 mil diameter spaced 30 to the inch and steel wire 7 mil diameter spaced 26 to the inch. The relative optical transparency was 77% and 65% respectively. The current transmitted by each anode was measured by a Faraday cup collector placed 0.5 cm behind the anode.
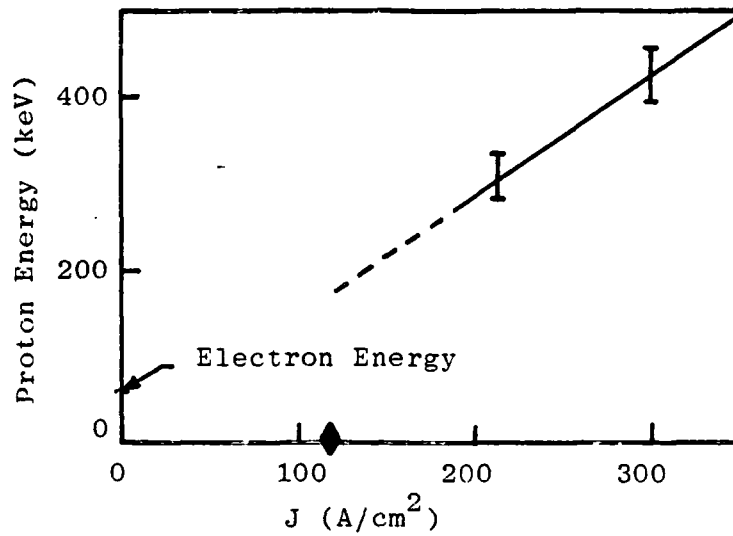
17

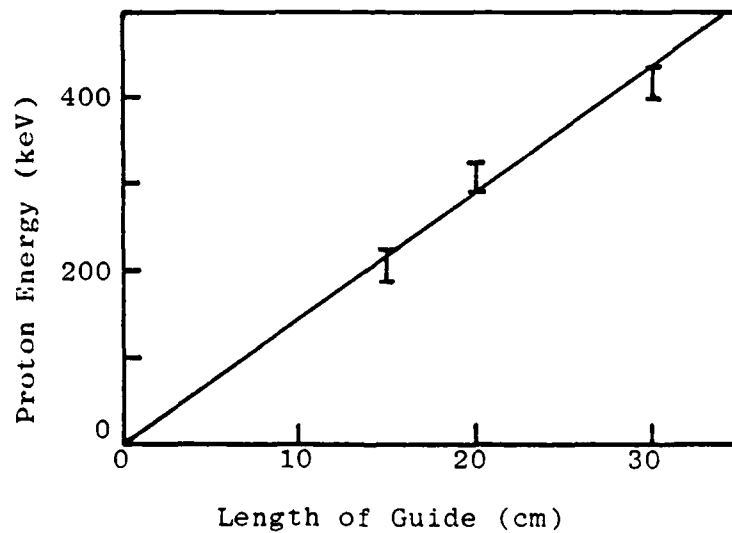Figure 8.   Proton Energy vs. Current Density.

Figure 9.   Proton Energy (From Time-of-Flight)
Measurements).

18

Peak transmitted currents were 7.8 kA for the tungsten mesh and 5.4 kA for the steel mesh, compared to 12 kA in the diode. The distribution of current was determined from witness plate patterns 0.1 cm behind the anode mesh. The average of $\vec{J}$ was uniform within ± 20% over the cathode area, and the pattern of anode wires was clearly visable. Changing the anode mesh did not change the diode current or voltage oscillograph traces within one line width. The electron energy spectrum and pulse width were not affected by the anode change.

The peak ion energy detected in a 30 cm long guide for each type of anode was plotted in Figure 8 as a function of the total injected current divided by the area of the guide, $\vec{J}$, to compare to experiments with larger diameter guides. The data implied that the peak ion energy scaled as the injected current at constant electron energy for a constant area guide provided $\vec{J}$ exceeded some threshold value. Since the depth of the potential well would not change at constant electron energy, the increase in ion energy was attributed to an increased current (or energy) density incident upon the guide walls. Note that the space change limited current was exceeded in all experiments, even those for low $\vec{J}$.

2.4   TESTS OF DIELECTRIC GUIDE GEOMETRY VARIATION

All of the dielectric guides used in this study were cylinders of acrylic plastic (polymethyl methacrylate). The wall thickness was either 0.32 cm or 0.64 cm, and three different sizes were used with an inner diameter of 1.9 cm, 5.7 cm. or 8.3 cm. The length of these guides was varied from 10 cm to 30 cm. All tests were run with cathodes having an outer diameter 0.6 to 0.7 cm smaller than the inner diameter of the guide used.

The effect of changing the diameter of the guide is shown in Figure 8 and has already been discussed in terms of changing the current density of the beam. Changing the ratio of the radii of the outer conducting wall (vacuum chamber diameter was 40 cm) to the radius of the guide by covering the outer surface of the guide with a conducting foil had no effect. Although the change affected the value of the limiting current (See equation 1, Section 4.2), the actual electron beam current injected was several times higher (by a factor of 10 to 100) than the limiting value, and the physical process was unchanged.

The effect of increasing the length of the dielectric guide is shown in Figure 9. The guide diameter was 5.7 cm and the electron beam propagated 30 cm to the end of the guide. The peak ion energy was observed to increase linearly with dielectric guide length out to a distance of 12 beam radii. This was the effect which makes this means of collective ion acceleration attractive -- it resembles a linear accelerator.

The thickness of the dielectric guide had no effect if it is greater than the electron range for peak diode voltage[5,18] and small compared to the diameter of the guide or the diameter of the conducting chamber walls.

SECTION III
EXPERIMENTS AT VEBA

An experiment in dielectric guide controlled collective ion acceleration was performed at Naval Research Laboratories, NRL[4]. The results demonstrate scaling of the phenomenon to higher energies. The experimental setup on the VEBA facility was:

- Lucite guide, 6.4 cm ID, 0.64 cm wall, 15 to 30 cm long.
- Steel vacuum chamber, 10.1 cm ID.
- Pointed cathode, 0.32 cm radius on 5.1 cm OD support.
- Foil anode, 12.5 μm Ti (also no anode tried).
- No magnetic field; in a vacuum of 10^{-4} torr.

The electron beam parameters were:

- Peak diode voltage = 1.5 MV
- Peak diode current = 75 kA
- Pulse length FWHM = 40 ns

The ion acceleration results are shown in Table 2.

An attempt to show the point of origin of the accelerated ions, by painting selective parts of a guide with CD_2, failed. The difference in counting rate was not detectable.

The dielectric guide surface was altered by cutting ribs into it (See Figure 10). This reduced the velocity of the

TABLE 2

ION ACCELERATION RESULTS AT VEBA

Ion Yield vs. Energy and Guide Length

Guide Length	Ion Energy	
	>4.2 Mev	>14 MeV
15 cm	3×10^{12}	10^{10}
30 cm	10^{12}	$<10^{9}$
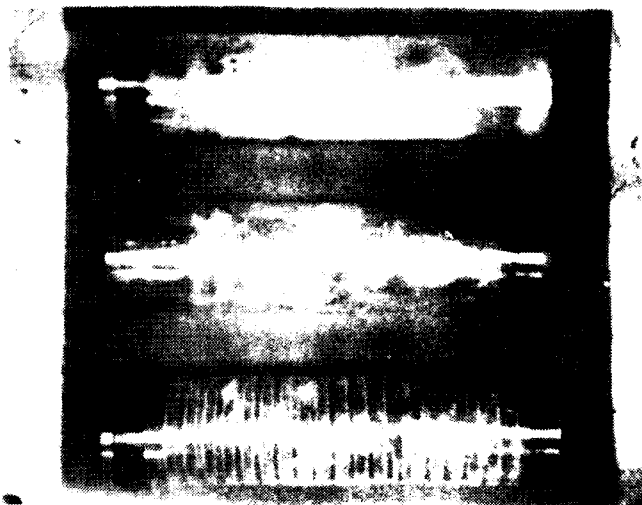
Figure 10.   Lucite Dielectric Guides used on VEBA.

23

electron beam front. Accelerated ions were detected, and the
peak energy was lower.

The VEBA experiment demonstrated that electron beam
transport in a dielectric guide was more efficient with larger
cathodes (6.7 cm diameter) while ion acceleration became more
efficient as the cathode diameter decreased to 0.32 cm.   The
transport variation was a function of beam energy injected axi-
ally into the guide, as the energy lost per unit length of di-
electric guide was constant[4].   Thus, although the smaller
cathodes accelerated ions more efficiently because the axial
current density was greater (see Figure 8), ions were not ac-
celerated over a distance of 30 cm (Table 2) because the cur-
rent density dropped below the cutoff. The diode and injection
geometry was not optimal.

The conclusions were:

- Collective ion acceleration in dielectric
  guides was demonstrated with higher energy
  beams.
- Control of the electron beam front velocity
  was demonstrated with guide design vari-
  ations.

SECTION IV
THEORETICAL MODEL

4.1 SUMMARY

Electron beam propagation and ion acceleration in a dielectric guide can be understood as space charge neutralization by ions emitted from the walls of the dielectric guide. At the start of the current pulse in hard vacuum, the electron beam is space charge limited and cannot propagate far beyond the anode mesh (1 cm typical, see Figure 2a). The beam blows up radially and impinges upon the guide walls. Surface flashover, initiated by trapped charge and space charge fields, causes the release of ions from the dielectric material. These ions are drawn towards the axis of the dielectric guide by the self-electric fields of the beam (Figure 2b). The ions provide partial neutralization of these electric fields and allow the beam to propagate further away from the anode (Figure 2c). The electric fields at the beam front accelerate some ions in the positive axial direction. The energy of these ions can exceed the maximum electron kinetic energy by following the motion of the beam front.

4.2 MODEL OF BEAM PROPAGATION

The theory of electron beam propagation through an ion layer[7] explains the general features of the experimental results and predicts scaling laws.

Propagation of an REB in vacuum is current limited by self space charge effects due to the potential drop from the wall (and cavity ends if $L/R \leq 2$) to the beam. This potential drop has to be less than the accelerating voltage of the electrons for the beam to move[8]. Assuming an electron beam

of uniform cross-section is injected into a dielectric tube of inner radius a and outer radius b and a dielectric constant ϵ, the space charge limiting current is[2]

$$I_\ell = \frac{mc^3}{e} \frac{(\gamma^{2/3}-1)^{3/2}}{1 + 2\ell n \frac{R}{r_b} + (1-\frac{1}{\epsilon}) 2\ell n \frac{a}{b}} \tag{1}$$

where R is the radius of the grounded, conducting, outer cylindrical shell, and r_b is the radius of the beam. Electron mass and charge are, respectively, m and $-e$, and c is the speed of light. For experiments at Spire an acrylic tube with a high frequency dielectric constant 2.8, a = 2.85 cm and b = 3.2 cm was inserted into an aluminum vacuum chamber with R = 10.1 cm. Assuming r_b = 2.8 cm and the maximum electron energy of 70 keV, $I_\ell \approx 133$ amperes. Since the peak injected current exceeds 9 kA and has a rise time less than 75 ns, the electron beam in Spire experiments was space charge limited in less than 1 ns.

The electron beam in a large aspect ratio diode can pinch to a small diameter. Theory[10] explains this pinching by very fast (10^9 cm/sec) motion of an ion layer that reduces the radial electric field.

The same idea is used here for a cylindrical geometry. Assume that an REB is injected axially into an evacuated cylinder, and spreads by self electric fields to the walls. Assume the walls generate a surface plasma. The electric field of the REB will push the plasma electrons into the wall and will pull the plasma ions into the chamber. The plasma ions will move radially and axially forward. Their presence in the drift chamber will reduce the electric field. The electric fields are maximized at the beam front and only the ions there will be accelerated to high velocities. Most of the plasma ions will generate an ion rich region near the wall. An electron rich region is found moving away from the wall.

26

When the ion layer near the walls has moved radially inward a sufficient amount, the electron beam front moves axially forward to a region where ions have not yet been generated. Here the process of ion generation and expansion of the ion layer starts again. No external fields are needed to guide the electron flow. Ions are believed to be generated by the surface flashover[5] of the acrylic dielectric used in experiments. An estimate of the speed of the ion sheath expansion and its effect on the propagation velocity of the REB front and ion acceleration can now be made using simple analytic models.

It should be noted that propagation through an ion layer is not space charge or magnetic field limited because both effects take place together. They cause a reduction in the electric field but do not cancel it all the way so that $\vec{E} \times \vec{B}$ drift takes place. This scheme of propagation and ion acceleration s shown to be limited by the amount of energy put into ion motion and into electric and magnetic fields. These rising fields may be used efficiently for collective acceleration of ion beams. Only simple estimates are derived here and further study is needed.

4.3   ION SHEATH MOTION ELECTRON AND ION TRAJECTORIES

Near the dielectric guide wall, the space charge field of the electron beam pulls the ions in a direction perpendicular to the cylindrical surface. The electric field parallel to the surface is shorted out by the plasma generated on this surface. Before ion motion takes place, the electric field near the cylindrical surface is given by

$$E_r{}^o = 60 \; \frac{I}{r} \; \langle \frac{1}{\beta_z} \rangle \tag{2}$$

27

where E_r is the radial electric field in volts/cm, I is the beam current (amperes), and r is the radius in cm.

Initially, electron motion takes place in a very thin layer near the guide surface. The thickness of this layer Δ, is estimated by assuming that the potential drop across it equals the voltage, V_o, that accelerated the electrons.

$$1/2 \ E_r^{\ o} \cdot \Delta = V_o \tag{3}$$

Without ions, electrons do not propagate in the axial direction. The self magnetic field force,

$$e \ \beta_z \ B_\Theta \quad \text{(where } B_\Theta = \frac{1}{5} \frac{I}{r} \text{ gauss)} \tag{4}$$

at the dielectric surface is less than the electric field force and the electrons are pushed into the wall.

Due to strong space charge fields and the bombardment of the wall by the electrons, plasma generation takes place. The plasma electrons are pushed radially outwards by the electric field while the ions are dragged inside. The magnetic field action on the ion motion may be neglected to first order. The ions move in the self consistent electric field that is equal to E_r^o of equation (2) at the ion front. As the ion sheath expands, its own space charge alters the electric field that accelerates the ions. The field drops gradually from E_r^o to zero if enough ions have been generated to screen the potential drop. The general long time behavior of the fields and ion motion is a problem for numerical computation; but for times that the ion sheath thickness, X^o, is much less than Δ of equation (3) the ion motion has been solved analytically[10]. At the front of the ion sheath the ions are accelerated by E_r^o. Hence:

$$X^O = \frac{1}{2} \frac{e Z E_r^O}{M} t^2 \qquad (5)$$

where eZ and M are ion charge and mass and the ion is acceler-
ated a distance X^O during the time t. All other ions are
accelerated by electric fields that change along the radial
direction, approximately linearly[10], but not in time
(assuming a constant current and electron energy beam), so that
a Lagrangian picture is easily applied. An ion situated half-
way from the ion front ($E = E_r^O$) to the wall plasma ($E = 0$)
is accelerated by the field $E = 1/2\ E_r^O$. The distance this
ion traverses in a time t is:

$$\frac{1}{2} \frac{eZ}{M} \frac{1}{2} E_r^O t^2 = \frac{1}{2} X^O$$

which states that this ion will be in the middle of the ion
sheath at all times. The ion density is thus a constant along
the sheath and its value is

$$eZ\ n_i = \frac{E_r^O}{4\pi X^O} = \frac{M}{2\pi eZ} t^{-2} \qquad (6)$$

where CGS units have been used, the density is in cm^{-3}.

In this constant density sheath the electric field drops
linearly to zero (the electron space charge inside the sheath
is neglected because $X^O << \Delta$). Very slight diamagnetic ef-
fects are caused by the ions, and the magnetic field inside the
ion sheath is equal to $I/(5r)$. The electron orbits are affect-
ed by the expanding ion sheath. Because the electric field is
reduced the magnetic field forces can reflect an electron mov-
ing outward from the REB backwards into the electron rich re-
gion. Electrons with grazing incidence will move parallel to
the dielectric surface, oscillating radially between the ion
sheath and the electron rich region. They

propagate axially until they reach a position where insuffi-
cient ion generation or ion sheath expansion took place. There
the above described phenomena occur and further propagation is
allowed.

The ion sheath thickness for electron reflection is cal-
culated by following an electron that enters the sheath with
radial velocity $V_r^o \ll c$. For simplicity, assume $\beta_z \approx 1$.
The motion of an electron inside the ion sheath is described by:

$$\gamma m \frac{dV_r}{dt} = e \left(E_r + \frac{V_r \times \beta_z}{c} \right) \tag{7}$$

Since the radial electric field E_r drops linearly from
E_r^o to zero in the ion sheath, the motion will be that of a
harmonic oscillator. From equation (7) and the value of B we
find that

$$d = \frac{\gamma m c^2}{e E_r^o} \cdot \left(\frac{V_r}{c} \right)^2 \tag{8}$$

This is the distance in which an electron will be reflected
(V_r becomes 0) in the ion sheath. For grazing incidence d is much
smaller than Δ. Using equations (3) and (8), in experiments
at Spire $d \approx 0.05$ cm for $V_o = 70$ kV and $I = 9$ kA. This as-
sumes that $V_r/c = 0.2$ and is only approximate since $\beta_z \approx 0.4$
and is not close to unity. The ion sheath expansion time t
would be 3.4 ns if $d \approx X^o$. Both t and d are small compared to
experimental parameters.

4.4   ION SOURCE

The velocity of propagation of the beam front, and that
of the associated ions, is limited by three different time
scales. The first is the time required to generate the ion
source. The second is the expansion time of the ion sheath to

a thickness large enough to allow further propagation. A third time scale is related to energy conservation considerations. The second and third time scales will be evaluated in section 4.7. This section covers generation of the ion source.

When the electron beam enters the dielectric guide and impinges upon the walls, ions are released. Three models of the ion emission mechanism are considered (Figure 11). Each physical mechanism evolves a gas at the surface of the material which is ionized by the beam.

The first process is surface heating which causes desorption of adsorbed gases as exhibited by metals exposed to an intense REB. The rate at which ions can be released from the surface of the material by this method is proportional to the beam current, but only weakly dependent upon electron energy. Higher energy particles penetrate further into the material, heating a greater volume with little change in surface temperature.

The time needed to generate the ion source when heating is the dominant process is calculated from the temperature required at the surface to cause desorption of surface material. To traverse an area ds the beam has to deposit a charge Q(V).dS, where Q(V) is the needed energy of electrons of V electron volts needed to heat a unit area for ion generation. The time dt is thus given by equating the power of the beam to the required heating:

$$dt = \frac{dS}{I} \cdot \frac{Q(V)}{V} \tag{9}$$

We thus arrive at the concept of areal velocity

$$V_a = \frac{1}{I} \frac{dS}{dt} = \frac{V}{Q(V)} \tag{10}$$
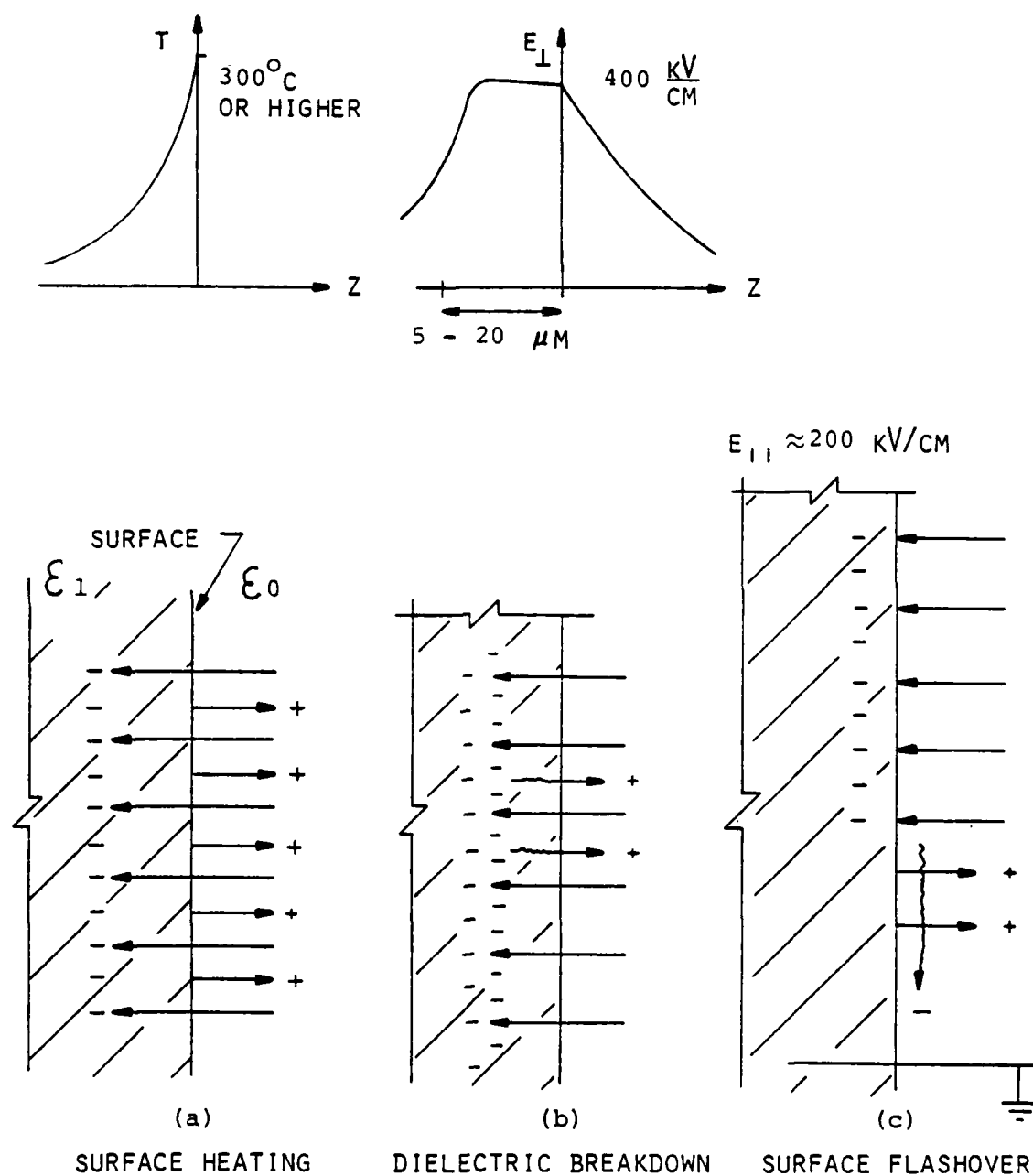
Figure 11.   How Ions Can be Released from Surface of Dielectric Material.

in cm^2/ (sec MA) as a reasonable measure of the rate at which ions can be released.

The concept of areal velocity is quite general and applies to ion release phenomena other than heating. The quantity $Q(V)$ need only be the number of electrons per unit area of energy V required to cause ion emission by any process with a threshold. The $Q(V)$ depends on the properties of the material. If this relationship holds, the areal velocity is constant for a given material provided the electron beam energy is constant.

For plastics, the areal velocity due to surface heating is expected to be on the order of 30 cm^2/nsMA from calculations.[11] This is two orders of magnitude below the measured velocity ($\sim$ 2000 cm^2/nsMA) for dielectric guides.

To explain the discrepancy, two additional mechanisms for the release of ions are proposed. The first considers dielectric breakdown or flashover on the surface of the material (Figure 11c). The second considers dielectric breakdown through the volume of the material (Figure 11b). In both cases the electron beam is assumed to impinge upon the guide wall some distance ahead of the neutralized region. A buildup of charge and electric field occurs.[12] This field initiates the emission of some ions directly.

The following surface flashover that neutralizes the electric field parallel to the guide heats a thin layer of material more efficiently than expected from the electron deposition profile. A dense plasma forms on the surface and

expands rapidly.[13] Approximately 10^{17} to 10^{18} ions/cm^2 of dielectric surface are released in this process as determined from pressure measurements after a shot. Evidence for surface flashover is seen in tracking patterns (Figure 12) on Lucite guide tubes.

In volume dielectric breakdown the electrons penetrating the dielectric material cause a buildup of trapped charge and create strong electric fields normal to the surface. Breakdown to the surface greatly enhances local conductivity in plastics. From experimental breakdown measurements with pulsed electron beams [14] the areal velocity of an REB in a Lucite guide would be about 250 cm^2/(nsMA). This is much faster than the rate calculated for heating but still an order of magnitude slow.

The mechanism which produces the high areal velocity in experiments is a combination of the three phenomena proposed.

- Surface flashover is the dominant process. SGEMP experiments[15] have shown that ion emission is significantly reduced if electric fields parallel to the surface are shorted out by fine wires.
- Surface heating occures. Melting of the lucite surface could be detected. Also, from reference 15, the peak current transported in a dielectric guide varied with the heat capacity of the material times the temperature rise to the melt point.
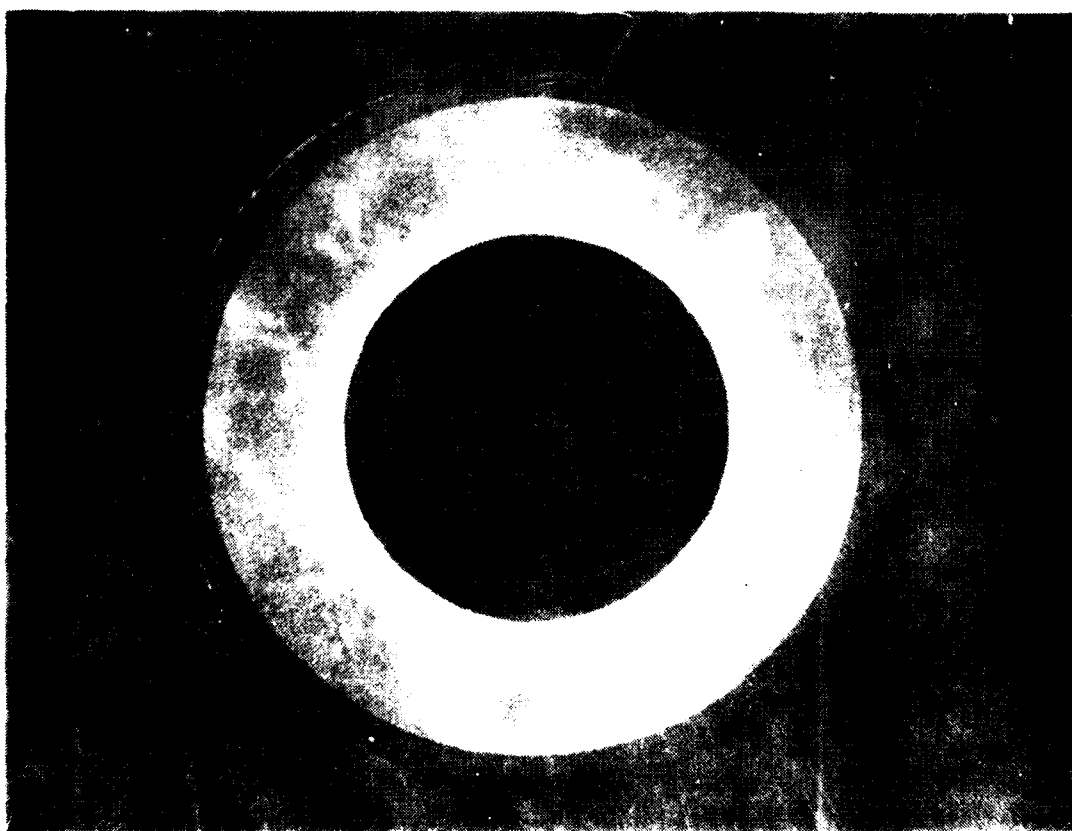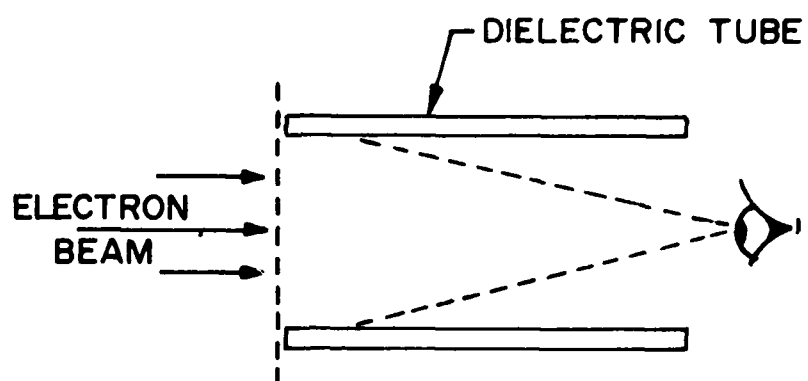
Figure 12.   Open Shutter Photograph of Surface Flashover
             On Dielectric Tube.

- Dielectric breakdown occurs since
  electron current transmission efficiency
  in a dielectric guide is reduced when the walls
  of the guide are thinner than the
  range of the relativisitic electrons
  in the material[5].

4.5 BEAM FRONT ACCELERATION AS A FUNCTION OF CURRENT

All of the mechanisms for the release of ions from a dielectric material predict that the number of ions created is proportional to electron beam current. This is consistant with the experiment. Assuming equation (10) is valid as the rate of ion release and beam front propagation, the acceleration of the beam front can be modeled as:

$$\frac{d^2 S}{dt^2} = V_a \frac{dI}{dt}$$

For a cylinder this gives:

$$2 \pi R a = V_a \frac{dI}{dt}$$

where a is the acceleration of the beam front, R is the radius of the guide, and dI is the rate of change of the electron beam current. For a slowly changing beam energy and $I = I_o t/t_r$, (approximately true for $t \leq 0.7\ t_r$ for diode geometries used in these experiments) equation (11) implies

$$a = \frac{V_a\ I_o}{2 \pi R t_r} \tag{12}$$

which is constant. The beam front and consequently the ions

trapped in the potential well should experience a constant acceleration. The data of Figure 9 provide a check of this model. If the acceleration is constant, then the ion energy would be proportional to the guide length. As shown, this is approximately true when the ions are not relativistic ($\beta \simeq 0.03$ maximum).

Two simple corrections can be made to equation (12). The current at the beam front is not exactly $I_o t/t_r$. It is reduced by:

- Transmission losses in the guide.
- Time of flight for electrons
- Relativisitic corrections.

Let t be the pulse width lost from the beam front to transport the beam and initiate ion emission. Using

$$Z = \text{guide length} = \frac{1}{2} \, at^2$$

then equation (12) implies

$$t = \frac{4\pi R t_r \, Z^{1/2}}{V_a I_o} \tag{13}$$

If the first correction is written as:

$$I = \frac{I_o}{t_r} \; t \; \exp \left(\frac{Z}{L}\right) \tag{14}$$

where I is the beam front current at position Z, then equation (14) becomes:

$$t = \left(\frac{4\pi R t_r L}{V_a I_o}\right)^{1/2} \left[\exp \left(\frac{Z}{L}\right) - 1 \right]^{1/2} \tag{15}$$

Here, L is the characteristic e-fold distance for current transport down the guide. Equation (15) reduces to equation (13) when $Z/L \ll 1$.

The time of flight correction can be written as:

$$I = \frac{I_o}{t_r} \quad (t - z/c) \tag{16}$$

This accounts for the time it takes the diode current to reach the beam front, assuming $\beta \approx 1$ for the beam electrons. An additional correction to I, time dilation, would be necessary if the velocity of the beam front was relativistic. Using equation (16), the value of Z in equation (13) can be written as:

$$Z/c = t + A(e^{-t/A} - 1) \tag{17}$$

$$A = \frac{2\pi R t_r c}{V_a I_o} \tag{18}$$

When t/A is small (true for these experiments), the first order correction to equation (17) cancels and equation (13) is recovered in second order.

4.6   COMPARISON TO EXPERIMENTAL RESULTS

Results at Spire (Figure 9) can be fit to equations (12) and (13), for the acceleration is constant with guide length The beam front velocity is low and transport length is small. The corrections are negligible (under 10%).

At VEBA[4] the beam front velocity and transport length were greater. The corrections are reasonable, and electron beam transport data fit within a factor of 2.

38

Assuming:

$$I_o = 75 \text{ kA}$$
$$t_r = 40 \text{ ns}$$
$$V_a = 2000 \text{ cm}^2/\text{mCoul}$$
$$L = 135 \text{ cm}$$
$$Z = 75 \text{ cm}$$
$$R = 3.18 \text{ cm},$$

Equation (13) yields t = 28 ns and equation (15) yields t = 38 ns, while equation (17) gives no change. About one half of the VEBA pulse, the rising current part, is lost to the guide wall.

4.7 OTHER LIMITS TO ION ACCELERATION

The propagation velocity of the electron beam front and ions trapped in the potential well is limited by the expansion time of the ion sheath. Assuming that the unneutralized electron rich region at the head of the beam has a thickness L_e, then L_e/t (expansion) gives the velocity of propagation. The expansion time is computed from the thickness of the ion sheath, d (equation 8), and the acceleration of ions at the inner edge of the sheath:

$$\frac{\gamma mc^2 \beta_r^2}{e E_r^o} = d = \frac{1}{2} \frac{e E_r^o}{M} t_{ex}^2 \tag{19}$$

$$t_{ex} = \frac{(2\gamma mc^2 Mc^2)^{1/2}}{e E_r^o c} \beta_r \tag{20}$$

The areal velocity is Le x 2 r/(t_{ex} = I) or

$$V_A \cong \frac{L_e \cdot 120\pi}{\beta_r \beta_z (\gamma)^{1/2}} \quad \frac{cm^2}{nsMA} \tag{21}$$

where L_e is in (cm). For REB which are highly space charge limited, $L_e \approx 1$ cm, and the radial velocity of the electron in the ion sheath is small, $\beta_r \approx 0.2$. For 1 MeV electrons, $V_A \approx 1500$ cm^2/(nsMA). For parameters of experiments at

39

Spire, V_A is greater. Thus, ion acceleration is not necessarily limited by this process as the areal velocity is comparable to that of surface flashover.

Ion acceleration can also be limited by energy considerations. The sum of the energy in electric and magnetic fields, that of the ions, and that delivered to the guide walls to create an ion source must be less than the total energy in the electron beam to allow propagation. The energy in the electromagnetic fields can be overestimated by assuming an infinitely long beam of uniform current density is propagating, unneutralized, in a conductive guide. These fields are not self-consistent at high currents. The guide radius equals the beam radius as the plasma near the dielectric guide is expected to be highly conducting.

$$E_r = \frac{2\ Ir}{R^2 \beta c} \qquad W_E = \frac{1}{8\pi} \quad \epsilon |E|^2$$

$$B_\Theta = \frac{2\ Ir}{R^2 c} \qquad W_B = \frac{1}{8\pi} \quad \frac{1}{\mu}|B|^2 \tag{22}$$

Here R is the beam radius, r is the radius at which the field has the given value, I is the current (CGS units) and W_E, W_B are energy densities. Integrating over the area $rdrd\Theta$, the total field energy per unit length is:

$$W/\ell = \frac{I_o^2}{4c^2} \qquad (1 + \frac{1}{\beta^2}) \tag{23}$$

In experiments at Spire, $W/\ell \approx 18$ J/M. This number can be compared to the energy delivered to the walls which is given by

$$W/\ell = 10^{-2}\ \pi R\ V_o \text{ (in MKS units)} \tag{24}$$

This has the approximate value $W/\ell < 33$ J/M at Spire. Assuming the energy in the ions is comparable to the total energy in the electromagnetic fields, ion acceleration was not limited by power in the fields, but by the energy lost to the wall.

As the experiment is scaled up in total energy, for high impedance diodes, the relative energy loss between the guide walls and the fields remains the same. For experiments at VEBA, for example, the energy in the fields was under 300 J/M while that lost to the wall exceeded 4 kJ/M. The important limit to this means of ion acceleration is the mechanism of ion emission from the dielectric guide wall.
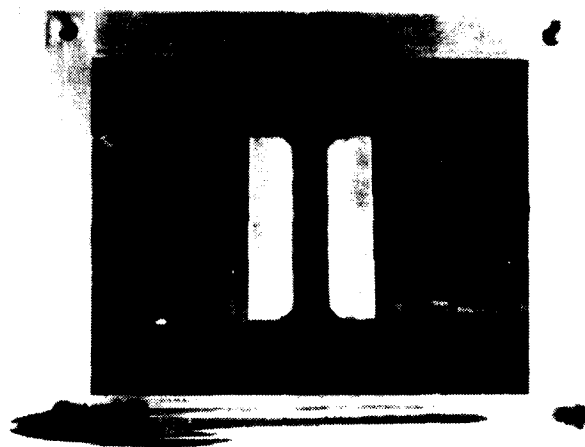
SECTION V
SPECTROMETER

Construction of a Thomson Parabola Mass Spectrometer[16] was a task under this contract. It was not available for experiments because its completion was delayed by the late award of contract and subsequent reduction in the originally proposed contract period.

The spectrometer is illustrated in Figure 13. It consists of the magnet and deflection plates, ion detector and detector power supply. The spectrometer was designed to fit into an available 14 inch ID auxillary vacuum chamber at Spire facilities. The chamber has been tested and can reach the 10^{-6} torr required operating pressure. The power supply has also been tested but not the ion detector.

The accuracy of this spectrometer is limited by beam spreading between the collimator and detector. Figure 14 gives the minimum detectable flux for given line widths assuming a 40 cm drift distance (adjustable in design). The electric field was designed to give a 3 mm deflection for 4 MeV ions. To achieve 10 precent accuracy ($\pm$ 0.3 mm) the incident flux would have to exceed 3×10^9 ions/cm^2 per pulse. To detect ions at this low level a CHEVERON* was chosen as the ion detector. Higher energies can be detected with longer drift regions.

---

*Galileo Electro-Optics Corp., Sturbridge, MA

DEFLECTION SYSTEM

DETECTOR

These parts are mounted in a Spire vacuum chamber.
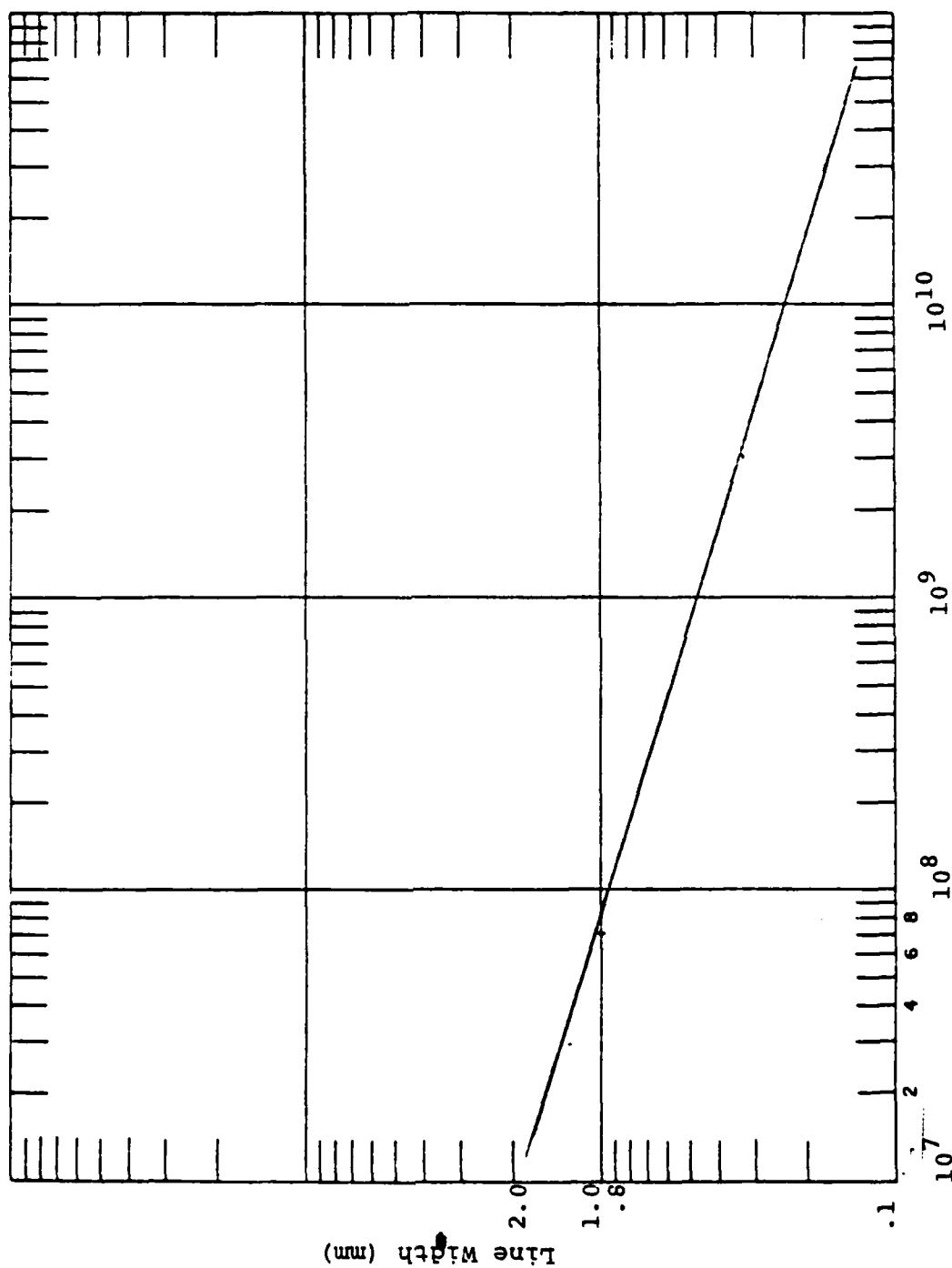
Figure 13.   Thomson Parabola Mass Spectrometer.

Figure 14. Spectrometer Detection Limit vs. Line Width.

Ions/cm^2 at Collimator

Line Width (mm)

44

SECTION VI
CONCLUSIONS

Experiments performed at Spire and at NRL have demonstrated dielectric guide controlled collective ion acceleration. Control of the phenomenon has been established by varying the electron beam parameters or guide geometry. Specifically, it has been shown that:

- Total electron current must exceed the space charge limit.
- Increasing electron current increases the ion energy.
- A minimum electron current density is required.
- Increasing guide length (assuming the electron beam can propagate to the end) increases ion energy.
- Increasing guide radius at constant electron current decreases ion energy.
- The energy or charge deposited per unit area of wall controls the velocity of propagation of the electron beam front and therefore the energy of the ions.

NRL VEBA results showed that:

- Dielectric guide controlled collective ion acceleration is effective at higher electron beam energies.

45

- An electron beam with current pinched on axis is more efficient for ion acceleration.
- Molding the surface of the guide can control the beam front velocity.

REFERENCES

1. See "Proceedings of the 1977 Particle Accelerator Confer-ence", IEEE Trans. on Nucl. Sci., NS-24, 1622-1670 (1977).

2. Robert B. Miller and David C. Straw, "Collective Ion Ac-celeration with Intense Relativistic Electron Beams", AFWL-TR-75-236 (1976).

3. C. L. Olsen et al., "Ionization Front Accelerator Feasi-bility Investigations", Proc. of the 2nd Int. Conf. on High Power Electron and Ion Beam Research and Technology, Cornell Univ. (1977).

4. J. A. Pasour et al., "Collective Ion Acceleration and Intense Electron Beam Propagation Within an Evacuated Dielectric Guide", Proc. of the 2nd Int. Conf. on High Power Electron and Ion Beam Research and Technology, Cornell Univ. (1977).

5. R. G. Little et al., "Cavity Current Enhancement by Di-electrics", IEEE Trans. on Nucl. Sci., NS-21, 249 (Dec. 1974).

    R. G. Little et al., "Cavity Current Enhancement by Di-electric Walls", IEEE Trans. on Nucl. Sci., NS-22, 2351 (1975).

6. A. Greenwald et al., "Electron Beam Transport in Dielec-trically Lined Cavities", Bull. Am. Phys. Soc., 21, 1147 (1976)

7. Private communication with Shyke Goldstein.

8. B. N. Brejzman and D. D. Ryutov, Nucl. Fusion 14, 873 (1974).

9. D. A. Hammer and N. Rostoker, "Propagation of High Cur-rent Relativistic Electron Beam", Phys. of Fluids 13, 1831 (1970).

10. S. Goldstein and Rosewell Lee, "Ion-Induced Pinch and the Enhancement of Ion Current by Pinched Electron Flow in Relativistic Diodes", Phys. Rev. Lett. 35, 1079 (1975).

11. A. E. Blaugrund and G. Cooperstein, "Intense Focusing of Relativistic Electrons by Collapsing Hollow Beams", Phys. Rev. Lett. 34, 461 (1974).

12. R. Little et al., "High Intensity Pulsed Electron Beam Energy Deposition in Solid Dielectrics", IEEE Trans. on Nucl. Sci. 16, No. 6, (Dec. 1969).

13. G. A. Vorober and V. S. Korolev, "Nanosecond Breakdown of Polymers", Sov. Phys. Tech. Phys. 21, 1222 (1976).

14 Rauch and Andrew, IEEE Trans. on Nuc. Sci. NS-13, No. 6, (109 (1966).

15. W. Seidler, Spire Corp., Bedford, MA, FR-20665 (1977) (unpublished).

16. G. W. Kuswa, "Electrostatic and Electromagnetic Confinement of Plasma and the Phenomenology of Relativistic Electron Beams", ANYAA9 Vol. 251, 514 (1975).

17. Galileo Electro-Optics Corp., Sturbridge, MA.

18. J. R. Uglum et al., "Electron Beam IEMP Simulation Development", Final Report for Contract DNA001-75-C-0136, Spire Corp., Bedford, MA. FR-75-10039 (1975).